**CHARACTERIZING STYLES OF VOLCANO GRAVITATIONAL DEFORMATION ON VENUS.** Rebecca M. Hahn[1] and Paul K. Byrne[1], [1]Department of Earth and Planetary Sciences, Washington University in St. Louis, St. Louis, MO 63130 (h.rebeccahahn@wustl.edu).

**Introduction:** Volcanoes are often unstable landforms and may undergo gravity-driven deformation that can alter the shape of the edifice. This phenomenon is common for both subaerial (e.g., Mount St. Helen, USA) [1,2] and submarine (e.g., Monowai, NZ) [3,4] volcanoes on Earth, as well as on Mars (e.g., Olympus Mons) [5]. Gravitationally deformed volcanoes have also been identified on Venus [6–8]. With a new global catalog of shield volcanoes containing ~85,000 edifices across Venus [9], we noted 182 edifices that appear to have undergone gravitational deformation. Structural and spatial analysis of these volcanoes can help quantify the types and possible drivers of volcano gravitational collapse on the second planet.

**Classification:** We classified those 182 volcanoes into one of four main deformation types based on the tectonic structures and landforms present: 1) landsliding; 2) sector collapse; 3) volcano spreading; and 4) volcano sagging. A fifth subset of edifices are those that are deformed in multiple styles or are otherwise difficult to classify with available data, and so we list them as "indeterminate".

Our first category includes those volcanoes with relatively small-scale and/or shallowly rooted downslope movements of material (≤1,000 km$^3$) on their flanks [1,2]; volcanoes with landslides are associated with backscarps, debris aprons, and stellate planforms [7,10,11] (**Figure 1a**). Sector-collapse volcanoes show large-scale (>1,000 of km$^3$) [4,12] down-slope movements of flank materials that often result in arc-shaped collapse scars [12,13], backscarps [13,14], and debris avalanche deposits [15,16] (**Figure 1b**). Volcano spreading results from the slow, outward movement of the edifice along a basal detachment [17–19], which produces radial graben on its flanks and folds and thrusts beyond the volcano's base [17,19,20] (**Figure 1c**). Volcano sagging occurs when the weight of the volcano down-flexes its basement [5,20], creating an edifice-encircling flexural trough and bulge with joints or graben along the flexural bulge, and outward-thrusting flank terraces on the edifice itself [5,19,21] (**Figure 1d**). Flank terraces are topographically subtle structures with a convex profile that resemble fish scales in plan view [19], and have been noted on volcanoes on Mars [5,22,23] and on Earth [5].

**Morphological Analysis:** Geospatial analysis and structural mapping of deformed volcanoes from our global catalog [9] was conducted with the Magellan SAR (synthetic aperture radar) FMAP (full-resolution radar map) left- and right-look global mosaics at 75 meter-per-pixel resolution (75 m/px) [24] in the ESRI ArcGIS Pro 2.7 environment. Mean deformed volcano diameter was calculated by averaging the long and short axes of each edifice, excluding any collapse related structures such as a debris apron. Deformation structures associated with each classification were either described in the attribute table, or by mapping the structures as polyline or polygon shapefiles in ArcGIS Pro. For example, debris aprons were mapped as polygon features and backscarps and concentric fractures were mapped as polylines (e.g., **Figure 1a**)

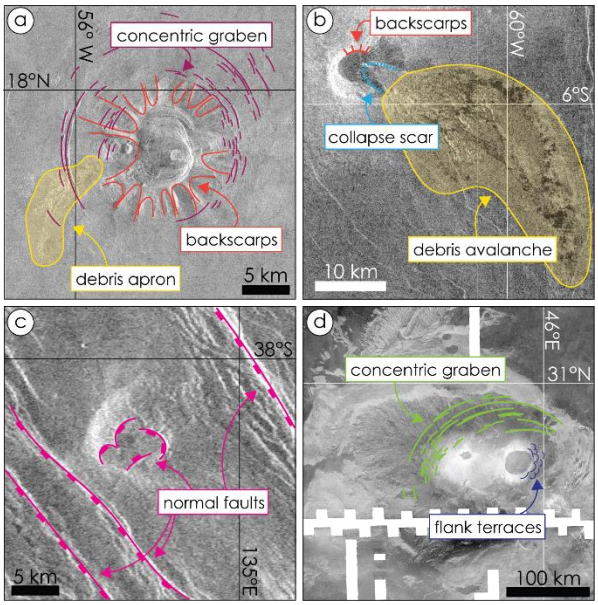


**Figure 1**: Examples of deformational structures associated with (**a**) landsliding, (**b**) sector collapse, (**c**) volcano spreading, and (**d**) volcano sagging. The radar look direction is from the left for each image, and each is shown in an equirectangular projection.

**Results & Discussion:** Initial summary statistics are given in **Table 1**. Overall, we note that nearly half of the deformed volcanoes on Venus are classified as indeterminate as they exhibit structures associated with multiple deformational styles, or the resolution of the Magellan SAR dataset is too low to accurately resolve deformation structures.

Very few volcanoes exhibit structures linked to volcano sagging and spreading. Those that display structures related to sagging (for example, the circumferential fractures and flank terraces on Tepev Mons in **Figure 1d**), are all >40 km in diameter, whereas those volcanoes that have undergone

**Table 1**
*Summary Statistics for Deformed Volcanoes*

| Deformation Type | Count ($n$ = 182) | Percent of Total | Mean Diameter (km) |
|---|---|---|---|
| *Landslide* | 49 | 27% | 34.4 ± 17.2 |
| *Sector Collapse* | 36 | 20% | 24.2 ± 12.6 |
| *Volcano Spreading* | 3 | 2% | 16.3 ± 3.8 |
| *Volcano Sagging* | 6 | 3% | 297 ± 273.6 |
| *Indeterminate* | 88 | 48% | 66.5 ± 90.9 |

landsliding, sector collapses, and volcano spreading are <40 km in diameter. This latter finding suggests that extensional gravitational deformation can affect edifices of all sizes, but that only the very largest volcanoes are sufficiently massive to downflex the underlying lithosphere. The smallest edifice we classified as "sagging" is ~50 km in diameter (centered at 19.21°N, 136.15°E). Although considerably smaller than all other volcanoes in this category (e.g., Tepev and Nyx Montes, which are 250 and 500 km in diameter, respectively), it is fully encompassed by the southern edge of Kamadhenu Corona and bounded by extensional structures. Coronae are widely accepted to have formed via mantle upwellings at the base of the lithosphere, causing an initial upwelling and subsequent flattening and gravitational relaxation that results in the characteristic annular structure [25,26]. Sagging structures (e.g., volcano-concentric fractures) related to this ~50 km diameter volcano could therefore be a consequence of the upwelling and relaxation of the corona. Alternatively, the presence of the corona and rift zones in this region likely resulted in a higher heat flux and a thinner elastic lithosphere, which in turn could have allowed this relatively modestly sized volcano to downflex its basement.

There are few instances of deformed volcanoes displaying structures associated with volcano spreading and, in all such instances, the volcanoes are <20 km in diameter. Typically, spreading occurs as a volcano grows, which exerts an increasing load on its substrata [17–19]. Structures linked to volcano spreading have been identified at Hawaii, the largest volcano on Earth [5], and even on the 150 km-diameter Martian volcano, Tharsis Tholus [17]. The small size of the volcanoes we identified as having structures linked to volcano spreading (e.g., normal faults cross cutting the flanks) may not actually have formed from the outward spreading of the edifice at all.

For example, at least one edifice that we classify as "spreading" is situated within a corona and bounded by rift zones (**Figure 1c**). These proximal structures suggest that the edifice may have experienced spreading not from the weight of the edifice itself but as a result of local extensional stresses associated with the nearby corona and rift zones. Furthermore, for a volcano to spread outward, the substrata must contain low-strength materials (e.g., clays, evaporates) [17–19]. The absence of water at the surface of Venus precludes the formation of a hydrated, low-permeability sediment layer suitable to produce detachment surfaces at the base of an edifice, at least in the present epoch [27]. It is therefore unlikely that a volcano on Venus will undergo volcano spreading along a shallow, low–strength layer. However, we do note structures associated with spreading (e.g., normal faults cross-cutting edifice flanks) on smaller edifices across Venus, which may contribute to our understanding of how small volcanoes respond to an increase in extensional stress at a scale greater than the edifice itself.

Volcanoes having undergone landsliding or sector collapses are more common than those associated with spreading and sagging (**Table 1**). The majority of volcanoes we classified as "landsliding" are located in the mid latitudes, with none at the north pole.

Proximal tectonic or volcanic structures may provide insight into the collapse mechanisms of deformed edifices. Of the 49 volcanoes showing landslides, 23% (11/49) are situated within a corona, again suggesting a genetic link between volcano deformation and coronae on Venus. Edifices classified as having undergone a sector collapse are geographically more widespread than those classified as "landsliding," with many "sector collapse" volcanoes extending to the high northern and southern latitudes. Several "sector collapse" volcanoes are linked to extensional structures, with 22% (8/36) within a rift zone. Of note, all edifices classified as "landsliding" or "sector collapse" are >500 km away from an impact crater, suggesting that volcano collapse is an endogenic process on Venus and not triggered by bolide strikes.

We note that structures associated with landslides, sector collapse, spreading, and sagging appear similar to those identified on deformed volcanoes on Earth, but there appears to be some variation in collapse mechanisms for different modes of volcano deformation (e.g., spreading volcanoes on Venus appear to be deformed by proximal extensional structures). To better evaluate these mechanism on Venus, detailed mapping of tectonic (e.g., rift zones) and volcanic (e.g., coronae) structures surrounding each deformed volcano in our catalog would help evaluate the role these features play in volcano collapse. Additionally, the analysis of gravity and topography data associated with large (>100 km in diameter) deformed volcanoes to estimate the thickness and flexibility of the underlying lithosphere, and the effects these lithospheric properties may have on volcano deformation, would help provide a framework for understanding how volcanoes evolve and deform on Venus in general.

**References:** [1] Chigira, M. (2002). Geomorphology, 46, 117–128. [2] Madonia, P. et al. (2019). Landslides, 16, 921–935. [3] Quartau, R. et al. (2010). Marine Geology, 275, 66–83. [4] Casalbore D. et al. (2020). International Journal of Earth Sciences, 109, 2643–2658. [5] Byrne, P.K. et al. (2013). Geology, 41, 339–342. [6] Guest, J.E. et al. (1992). JGR:P, 97, 15949–15966. [7] Bulmer, M.H. & Wilson, J.B. (1999). EPSL, 171, 277–287. [8] Ivanov, M.A. & Head, J.W. (1999). JGR:P, 10, 18907–18924. [9] Hahn, R.M & Byrne, P.K. (2022). WUSTL digital data repository. [10] Pavri, B. et al. (1992). JGR:P, 97, 13445–13478. [11] Bridges, N.T. (1995). GRL, 20, 2781–2784. [12] Romero, J.E. et al. (2021). Frontiers in Earth Sciences, 9, 639825. [13] Coombs, M.L. et al. (2007). USGS. [14] Martinez-Moreno, F.J. et al. (2018). JVGR, 357, 152–162. [15] Capra, L. et al. (2002). JVGR, 113, 81–110. [16] Bernard, B. et al. (2008). JVGR, 176, 36–43. [17] Borgia, A. et al. (2000). AREPS, 28, 539–570. [18] Marquez , A. et al. (2008). GRL, 35. [19] Byrne, P.K. et al. (2009). EPSL, 281, 1–13. [20] de Vries, B.V.W & Davies, T. (2015). The Encyclopedia of Volcanoes: Academic Press. [21] Kervyn M. et al. (2010). Geosphere, 6, 482–498. [22] Carr, M.H. et al. (1977). JGR, 82, 3985–4015. [23] Thomas, P.J. et al. (1990). JGR:SE, 95, 14345–14355. [24] Ford (1993). Guide to Magellan image interpretation. [25] Pronin, A.A. & Stofan, E.R. (1990). Icarus, 87, 452–474. [26] Gülcher, A.J.P. et al. (2020). Nature Geoscience, 13, 547–554. [27] McGovern, P.J. & Solomon, S.C. (1998). JGR:P, 103, 11071–11101.